
Imaging in random acoustic waveguides

Liliana Borcea

Computational and Applied Mathematics

Rice University

borcea@caam.rice.edu

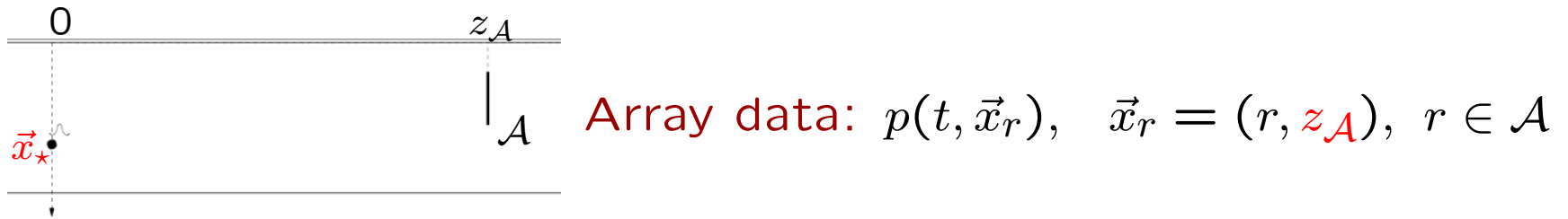
Collaborators:

Leila Issa, Computational and Applied Mathematics, Rice.

Chrysoula Tsogka, Mathematics, University of Crete.

Support: ONR: N00014-05-1-0699; N00014-09-1-0290
NSF: DMS-0604008; DMS-0934594, DMS-0907746.

Source localization with passive array of receivers



Problem: Determine source location $\vec{x}_* = (x_*, 0)$ (source cross-range x_* and the range z_A to the array).

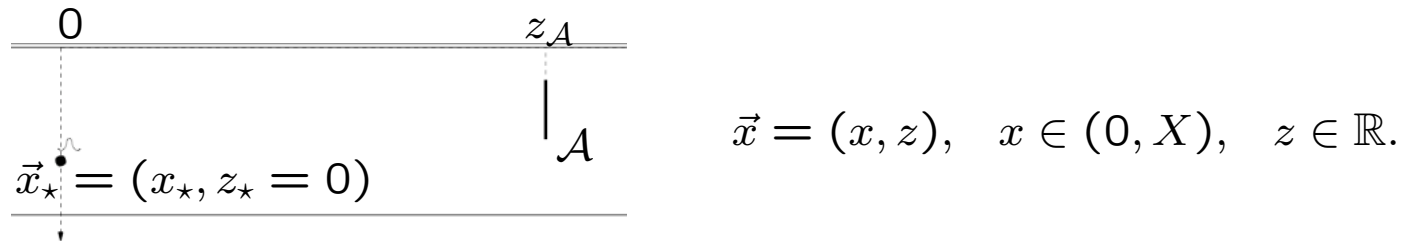
- This is the simplest imaging problem. Can be extended to imaging reflectors with active arrays of sources and receivers.

Difficulty: We consider waveguides with **fluctuating sound speed**. The fluctuations are typically small (1% – 3%) but their cumulative long range effect is strong \rightsquigarrow $p(t, \vec{x}_r)$ **loses coherence**.

Goal of talk

- Using mathematical analysis based on **modeling** the wave speed fluctuations with **random processes**:
 1. Understand how the pressure field received at the array loses coherence \rightsquigarrow how and why widely used imaging methods fail.
 2. Show how imaging can still be done with incoherent data.

Mathematical setup. Planar waveguide.



$$-\frac{1}{c^2(\vec{x})} \frac{\partial^2 p(t, \vec{x})}{\partial t^2} + \Delta p(t, \vec{x}) = f(t) \frac{\partial}{\partial z} \delta(\vec{x} - \vec{x}_*),$$

$$p(t, \vec{x}) \equiv 0, \quad t \leq 0$$

$$p(t, \vec{x}) = 0, \quad x \in \{0, X\}.$$

- The sound speed model is*

$$\frac{c_o^2}{c^2(\vec{x})} = 1 + \varepsilon \nu(\vec{x}), \quad \varepsilon \ll 1$$

$\nu(\vec{x})$ is a bounded, mean zero random process, stationary and decorrelating fast enough in z .

*For simplicity $c_o = \text{constant}$ but $c_o(x)$ could be considered. Typical $\varepsilon = 1-3\%$

Step 1: Write the mathematical model of the data recorded at the array: $p(t, \vec{x}_r)$ for $\vec{x}_r = (r, z_{\mathcal{A}})$ and $r \in \mathcal{A}$.

Unperturbed waveguides ($\varepsilon = 0$)

- We have $p(t, \vec{x}) = \int \frac{d\omega}{2\pi} \hat{p}(\omega, \vec{x}) e^{-i\omega t}$ where

$$\left(\frac{\omega^2}{c_o^2} + \frac{\partial^2}{\partial x^2} \right) \hat{p}(\omega, \vec{x}) + \frac{\partial^2 \hat{p}(\omega, \vec{x})}{\partial z^2} = \hat{f}(\omega) \delta(x - x_*) \delta'(z)$$

$$\begin{aligned} \hat{p}(\omega, \vec{x}) &= 0 \quad \text{for } x \in \{0, X\}, \quad \vec{x} = (x, z), \\ \hat{p}(\omega, \vec{x}) &= \text{bounded \& outgoing at } z \rightarrow \pm\infty. \end{aligned}$$

- Separation of variables \rightsquigarrow solution in terms of eigenfunctions*

$$\phi_j(x) = \sqrt{\frac{2}{X}} \sin\left(\frac{\pi j x}{X}\right) \quad \text{for } j = 1, 2, \dots \quad \text{and eigenvalues}$$

$$\mu_j = \left(\frac{\omega}{c_o}\right)^2 - \left(\frac{\pi j}{X}\right)^2 = \left(\frac{2\pi}{\lambda}\right)^2 \left[1 - \left(\frac{j\lambda}{2X}\right)^2\right], \quad \frac{\omega}{c_o} = \frac{2\pi}{\lambda}.$$

*If $c_o = c_o(x)$ \rightsquigarrow slight complication that ϕ_j are frequency dependent.

Data model at receiver $\vec{x}_r = (r, z_A)$ in unpert. waveguide

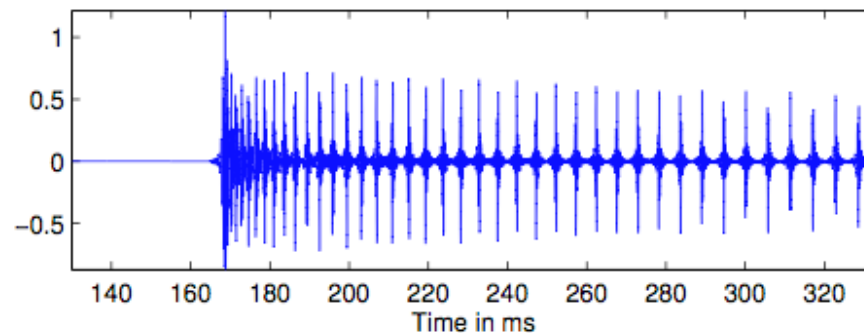
$$\hat{p}(\omega, \vec{x}_r) = \frac{\hat{f}(\omega)}{2} \left[\sum_{j=1}^{N(\omega)} \phi_j(x_*) \phi_j(r) e^{i\beta_j(\omega)z_A} + \underbrace{\sum_{j>N(\omega)} \phi_j(x_*) \phi_j(r) e^{-\beta_j(\omega)z_A}}_{\text{evanescent}} \right]$$

with modal wavenumbers

$$\beta_j(\omega) = \begin{cases} \frac{2\pi}{\lambda} \sqrt{1 - \left(\frac{j\lambda}{2X}\right)^2}, & j = 1, \dots, N(\omega) = \left\lfloor \frac{2X}{\lambda} \right\rfloor \\ \frac{2\pi}{\lambda} \sqrt{\left(\frac{j\lambda}{2X}\right)^2 - 1}, & j > N(\omega). \end{cases}$$

Numerics*

$p(t, \vec{x}_r)$



*Setup: $c_o = 1.5\text{km}$, pulse bandwidth 1.5 – 4.5kHz ($\lambda_c = 0.5\text{m}$). The waveguide is $20\lambda_c$ deep and $z_A = 494\lambda_c$.

Model in random waveguides

$$\left[\frac{\omega^2}{c_0^2} + \frac{\partial^2}{\partial x^2} + \varepsilon \nu(\vec{x}) \frac{\omega^2}{c_0^2} \right] \hat{p}(\omega, \vec{x}) + \frac{\partial^2 \hat{p}(\omega, \vec{x})}{\partial z^2} = \hat{f}(\omega) \delta(x - x_*) \delta'(z)$$

- For each z we can expand $\hat{p}(\omega, \vec{x})$ in orthonormal basis $\{\phi_j(x)\}_{j \geq 1}$

$$\hat{p}(\omega, \vec{x}) = \sum_{j=1}^{N(\omega)} \phi_j(x) \left[a_j(\omega, z) e^{i\beta_j(\omega)z} + b_j(\omega, z) e^{-i\beta_j(\omega)z} \right] + \sum_{j > N(\omega)} \phi_j(x) \hat{P}_j^e(\omega, z)$$

- Here a_j , b_j and \hat{P}_j^e satisfy a coupled system* of stochastic ODE's driven by stationary random processes

$$C_{j,l}(z) = \int_0^X dx \nu(\vec{x}) \phi_j(x) \phi_l(x), \quad j, l = 1, 2, \dots \quad \vec{x} = (x, z).$$

*Kohler, Papanicolaou-1977; Garnier, Papanicolaou - 2007

Model in random waveguide

$$\begin{aligned} (\partial_z^2 + \beta_j^2) (a_j e^{i\beta_j z} + b_j e^{-i\beta_j z}) + \varepsilon \left(\frac{\omega}{c_0}\right)^2 \sum_{l=1}^N C_{jl} (a_l e^{i\beta_l z} + b_l e^{-i\beta_l z}) \\ + \varepsilon \left(\frac{\omega}{c_0}\right)^2 \sum_{l>N} C_{jl} \hat{P}_l^\varepsilon = 0, \quad j = 1, \dots, N, \end{aligned}$$

$$(\partial_z^2 - \beta_j^2) \hat{P}_j^\varepsilon + \varepsilon \left(\frac{\omega}{c_0}\right)^2 \left[\sum_{l=1}^N C_{jl} (a_l e^{i\beta_l z} + b_l e^{-i\beta_l z}) + \sum_{l>N} C_{jl} \hat{P}_l^\varepsilon \right] = 0.$$

- **Boundary cond:** $a_j(\omega, z = 0)$ and $\hat{P}_j^e(\omega, z = 0)$ given by source excitation. As $z \rightarrow \infty$, the field is outgoing and $\hat{P}_j^\varepsilon(\omega, z) \rightarrow 0$.
- To get well posed problem ask*: $(\partial_z a_j) e^{i\beta_j z} + (\partial_z b_j) e^{-i\beta_j z} = 0$.
- Eliminating the evanescent $\hat{P}_j^e(\omega, z) \rightsquigarrow$ **closed first order system** for $\{a_j(\omega, z), b_j(\omega, z)\}_{j=1, \dots, N(\omega)}$ driven by **random** $\{C_{jl}(z)\}$.

*Kohler, Papanicolaou-1977; Garnier, Papanicolaou - 2007

Model in random waveguides

- The stochastic ODE system is studied with the **asymptotic** ($\varepsilon \rightarrow 0$) limit tools of Khasminskii, Blakenship, Papanicolaou, Stroock, Varadhan.
 - For ranges $\ll O(\varepsilon^{-2})$ the fluctuations are negligible.
 - The fluctuations play a role at ranges $\sim O(\varepsilon^{-2})$
 - As $\varepsilon \rightarrow 0$, negligible coupling between a_j and b_j for smooth z-autocorrelation of fluctuations \rightsquigarrow **forward scattering approx***.
- \rightsquigarrow **Closed first order system of stochastic ODE's for $\{a_j\}_{j=1,\dots,N(\omega)}$**

*Kohler, Papanicolaou-1977

The random transfer matrix (Green's function) $T_{jl}^\varepsilon(\omega, z)$

$$a_j(\omega, z/\varepsilon^2) \approx \sum_{l=1}^{N(\omega)} T_{jl}^\varepsilon(\omega, z) a_l(\omega, 0), \quad a_l(\omega, 0) = \frac{\hat{f}(\omega)}{2} \phi_l(x_\star),$$

where

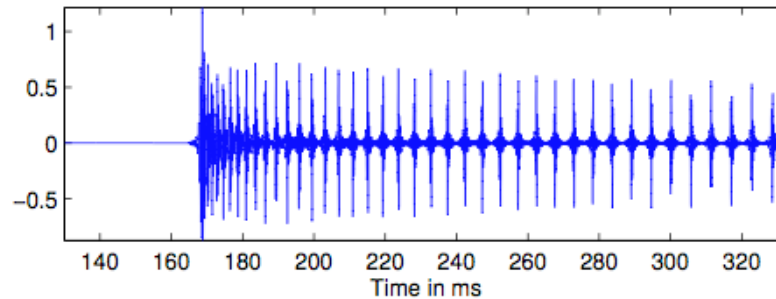
$$\begin{aligned} \frac{\partial}{\partial z} T^\varepsilon(\omega, z) &= \left[\frac{1}{\varepsilon} \mathbb{P} \left(\omega, \frac{z}{\varepsilon^2} \right) + \mathbb{E} \left(\omega, \frac{z}{\varepsilon^2} \right) + \dots \right] T^\varepsilon(\omega, z), \quad z > 0, \\ T^\varepsilon(\omega, 0) &= I. \end{aligned}$$

- Leading coupling: $\mathbb{P}_{jl}(\omega, z) = \frac{i}{2} \left(\frac{\omega}{c_0} \right)^2 \frac{C_{jl}(z)}{\beta_j(\omega)} e^{i[\beta_l(\omega) - \beta_j(\omega)]z}$
- The second order coupling is via the evanescent modes

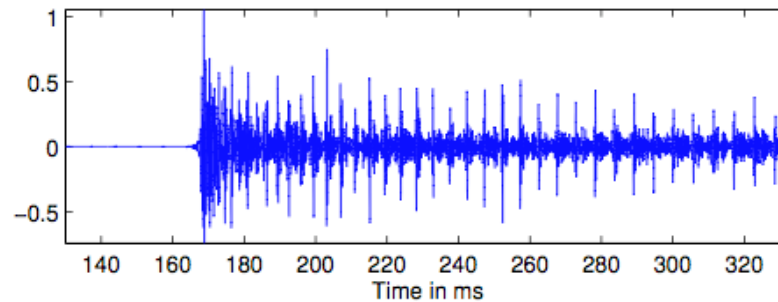
$$\mathbb{E}_{jl}(\omega, z) = \frac{i}{4} \left(\frac{\omega}{c_0} \right)^4 \sum_{l' > N} \int_{-\infty}^{\infty} ds \frac{C_{jl'}(z) C_{ll'}(z+s)}{\beta_{l'}(\omega) \beta_j(\omega)} e^{i\beta_{l'}(\omega)(z+s) - i\beta_j(\omega)z - \beta_{l'}(\omega)|s|}$$

Data model in random waveguides*

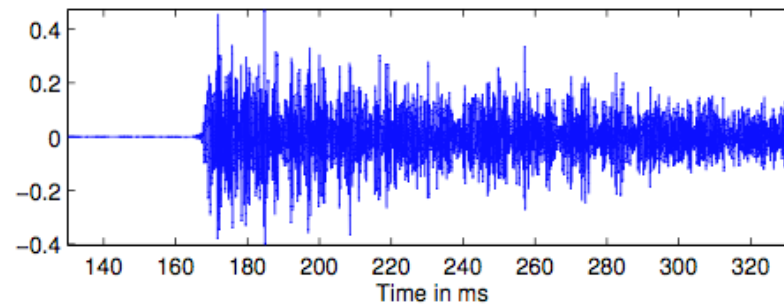
$$p(t, r, z_{\mathcal{A}} = Z/\varepsilon^2) \approx \int \frac{d\omega}{2\pi} \frac{\hat{f}(\omega)}{2} \sum_{j,l=1}^{N(\omega)} T_{jl}^{\varepsilon}(\omega, Z) \phi_l(x_{\star}) \phi_j(r) e^{i\beta_j(\omega)z_{\mathcal{A}} - i\omega t}$$



$\varepsilon = 0\%$



$\varepsilon = 1\%$



$\varepsilon = 3\%$

*Speed fluctuates about $c_0 = 1.5\text{km}$, with correlation length $= \lambda_c = 0.5\text{m}$. Pulse bandwidth 1.5 – 4.5kHz. The waveguide is $20\lambda_c$ deep and $z_{\mathcal{A}} = 494\lambda_c$.

Statistics of the array data

$$p(t, r, z_{\mathcal{A}} = Z/\varepsilon^2) \approx \int \frac{d\omega}{2\pi} \frac{\hat{f}(\omega)}{2} \sum_{j,l=1}^{N(\omega)} T_{jl}^{\varepsilon}(\omega, Z) \phi_l(x_{\star}) \phi_j(r) e^{i\beta_j(\omega)z_{\mathcal{A}} - i\omega t}$$

- As $\varepsilon \rightarrow 0$, $T^{\varepsilon}(\omega, z)$ converges in distribution* to a Markov diffusion process with generator computed explicitly in terms of correlation function of fluctuations.

- All statistical moments of $T^{\varepsilon}(\omega, z)$ can be computed approximately for $\varepsilon \ll 1$.

*Kohler, Papanicolaou - 1977.

Step 2: Analyze coherent part of array data $E \{p(t, \vec{x}_r)\}$.

This is what imaging methods rely on.

The coherent field

$$E \{p(t, r, z_A)\} \approx \int \frac{d\omega}{2\pi} \frac{\hat{f}(\omega)}{2} \sum_{j,l=1}^{N(\omega)} E \{T_{jl}^\varepsilon(\omega, Z)\} \phi_l(x_\star) \phi_j(r) e^{i\beta_j(\omega)z_A - i\omega t}$$

where $z_A = Z/\varepsilon^2$ and $\lim_{\varepsilon \rightarrow 0} E \{T_{jl}^\varepsilon(\omega, Z)\} = \delta_{jl} e^{-\mathcal{D}_j(\omega)Z + i\mathcal{O}_j(\omega)Z}$.

- $\mathcal{D}_j(\omega) > 0$ (power spectral densities of fluctuations) is due entirely to direct coupling of propagating modes.
- $\mathcal{O}_j(\omega)$ is also caused by coupling via evanescent modes (they carry negligible energy but cause dispersion).
- The coherent field decays exponentially with range.

The mean intensity and frequency decorrelation

- To compute intensity $E \left\{ p^2 \left(t, r, z_{\mathcal{A}} = Z/\varepsilon^2 \right) \right\}$ we need second moments $E \left\{ T_{jl}^\varepsilon(\omega, Z) \overline{T_{j'l'}^\varepsilon}(\omega', Z) \right\}$.

- We have frequency decorrelation for $|\omega - \omega'| \gg O(\varepsilon^2)$

$$E \left\{ T_{jl}^\varepsilon(\omega, Z) \overline{T_{j'l'}^\varepsilon}(\omega', Z) \right\} \approx E \left\{ T_{jl}^\varepsilon(\omega, Z) \right\} E \left\{ \overline{T_{j'l'}^\varepsilon}(\omega', Z) \right\}.$$

- For nearby frequencies $\omega' = \omega - \varepsilon^2 h$,

$$\int \frac{dh}{2\pi} E \left\{ T_{jl}^\varepsilon(\omega, Z) \overline{T_{j'l'}^\varepsilon}(\omega - \varepsilon^2 h, Z) \right\} e^{i \left[\beta_j(\omega) - \beta_{j'}(\omega - \varepsilon^2 h) \right] z_{\mathcal{A}} - iht} \approx$$

$$\delta_{jj'} \delta_{ll'} \mathcal{W}_j^{(l)}(\omega, t, Z) + (1 - \delta_{jj'}) \delta_{jl} \delta_{j'l'} \text{ exp. decay in } Z.$$

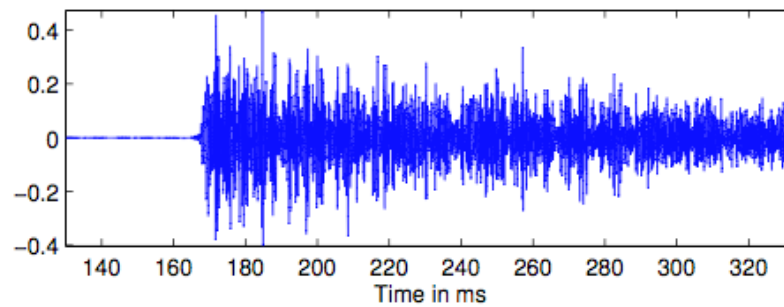
The loss of coherence

- The Wigner transform $\mathcal{W}_j^{(l)}(\omega, t, Z)$ dominates at long ranges and the intensity of the field recorded at $\vec{x}_r = (r, z_A = Z/\varepsilon^2)$ is

$$E \{ p^2(t, r, z_A) \} \approx \varepsilon^2 \int \frac{d\omega}{2\pi} \frac{|\hat{f}(\omega)|^2}{4} \sum_{j,l=1}^{N(\omega)} \mathcal{W}_j^{(l)}(\omega, t, Z) \phi_l^2(x_*) \phi_j^2(r)$$

- In spite of the ε^2 factor, $E\{p^2\} \gg |E\{p\}|^2$ at long ranges, because the latter decays **exponentially**.

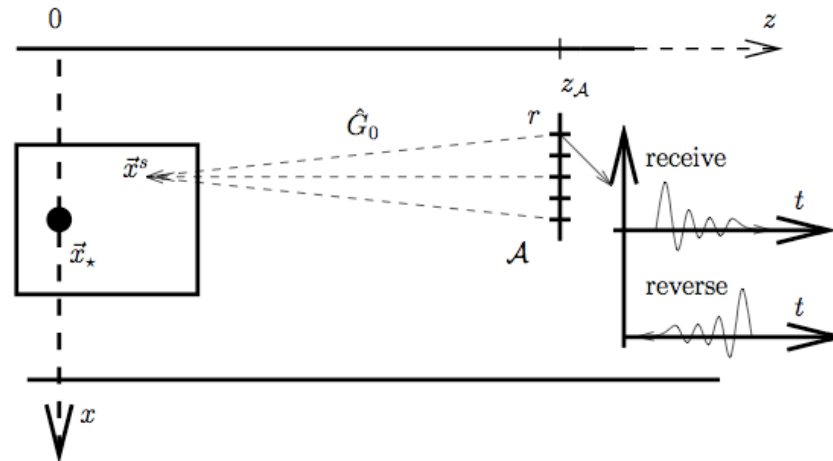
The **incoherent field** $p - E\{p\}$ becomes dominant at long ranges.



$$\varepsilon = 3\%$$

Step 3: Analyze how typical imaging methods fail.

Source localization using “time reversal”



$$\mathcal{I}^{\text{TR}}(\vec{x}^s) = \int d\omega \int_A dr \bar{p}(\omega, \vec{x}_r) \underbrace{\hat{G}_0(\omega, \vec{x}_r; \vec{x}^s)}_{\text{Green's function}}$$

- We evaluate the imaging function at points $\vec{x}^s = (x^s, z^s)$ in a search domain and estimate \vec{x}_* as the peak of \mathcal{I}^{TR} .

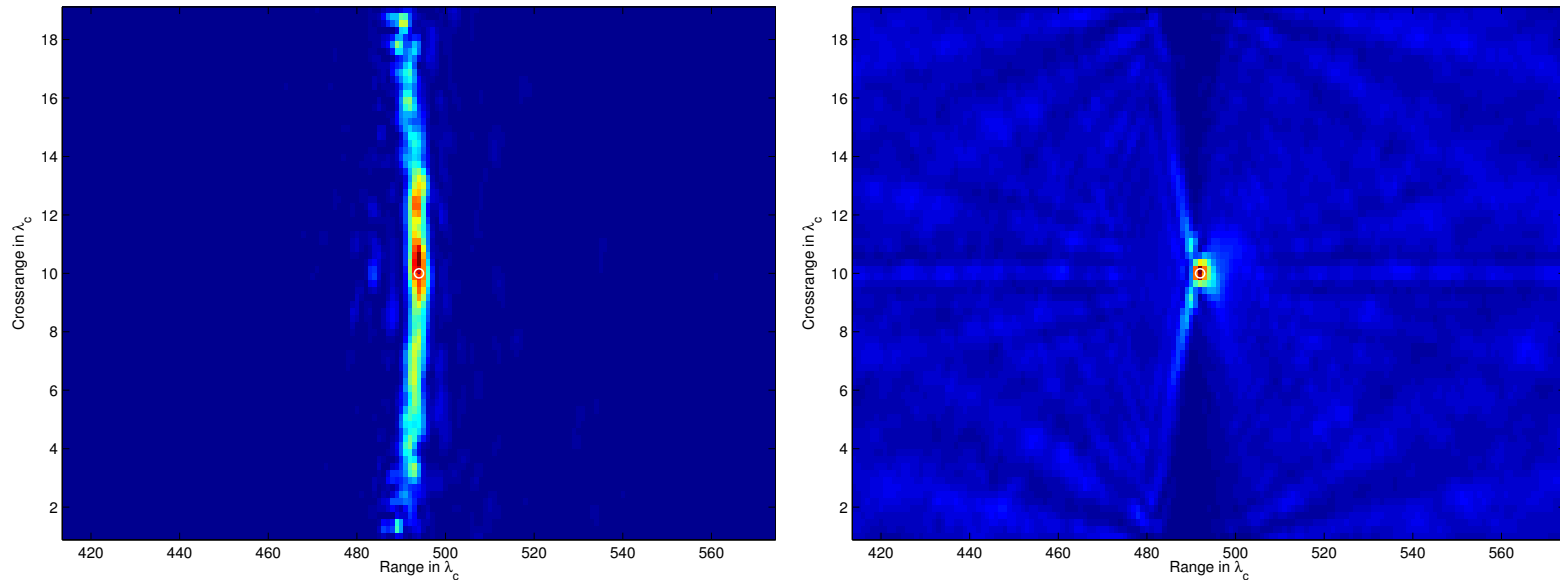
Expected to focus at \vec{x}_* by time reversibility of the wave equation, at least for large enough apertures and if \hat{G}_0 is a good enough approximation of the backpropagation in the real medium.

Matched Field (MF) methods

$$\mathcal{I}^{\text{MF}}(\vec{x}^s) = \int d\omega \left| \int_{\mathcal{A}} dr \bar{p}(\omega, \vec{x}_r) \hat{G}_0(\omega, \vec{x}_r; \vec{x}^s) \right|^2$$

- This is the conventional (Bartlett) MF function. It is known to be more robust than the previous method.
 - **Variants of MF** that use additional data filtering techniques are widely used and have slightly better performance in practice.
 - They deal well with additive noise, but rely on coherent data.
- ↪ sooner or later they will fail similarly at long ranges.

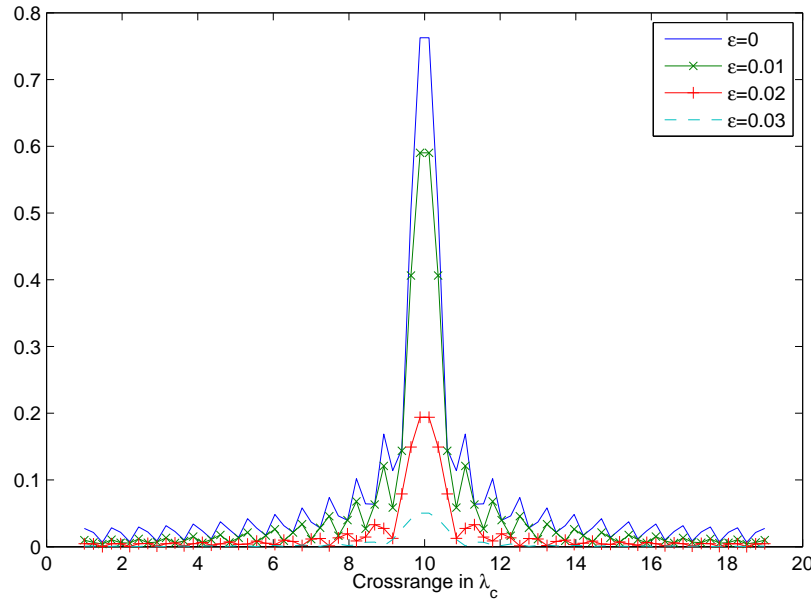
Illustration in media with negligible fluctuations



- The imaging functions are computed at 70% aperture and frequency band $2 \pm 0.375\text{kHz}$. The source is in the center.

Next: Let us see what happens when the fluctuations play a role.

Mean of $\mathcal{I}^{\text{TR}}(\vec{x}^s)$ focuses but method statistically unstable



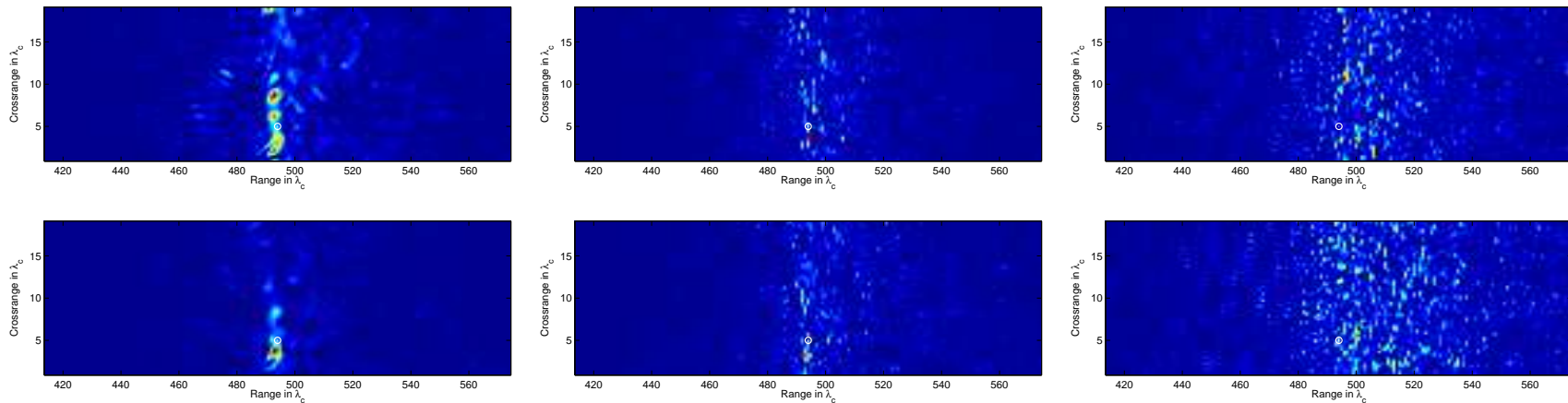
$$|E \{ \mathcal{I}^{\text{TR}}(\vec{x}_*) \} | \leq C e^{-\mathcal{D}_1(\omega_c)Z}.$$

The relative standard deviation* grows exponentially with range.

$$\frac{\sqrt{E \{ |\mathcal{I}^{\text{TR}}(\vec{x}_*)|^2 \} - |E \{ \mathcal{I}^{\text{TR}}(\vec{x}_*) \}|^2}}{|E \{ \mathcal{I}^{\text{TR}}(\vec{x}_*) \}|} \geq \frac{\varepsilon \sqrt{\omega_c/B}}{\sqrt{N(\omega_c)}} e^{\mathcal{D}_1(\omega_c)Z} \underbrace{\mathcal{F}(\omega_c, Z, x_*)}_{\text{algebraic in } Z}$$

*The frequency band is $|\omega - \omega_c| \leq B$.

Numerical results



Full aperture. Left: $\varepsilon = 2\%$, bandwidth: $2 \pm 0.375\text{kHz}$. Middle: $\varepsilon = 2\%$ and full bandwidth. Right: $\varepsilon = 3\%$ and full bandwidth.

- Even though the statistical mean focuses in theory, we cannot observe it due to the statistical instability.

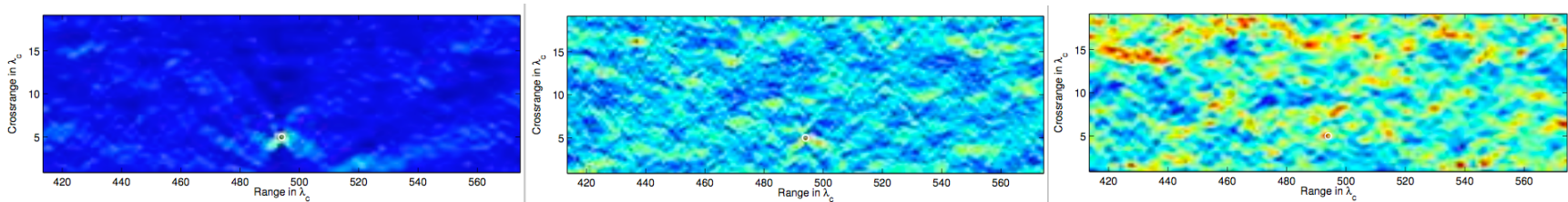
Matched Field

$$E\{\mathcal{I}^{\text{MF}}(\vec{x}^s)\} = \int d\omega E \left\{ \left| \int_{\mathcal{A}} dr \bar{\hat{p}}(\omega, \vec{x}_r) \hat{G}_0(\omega, \vec{x}_r; \vec{x}^s) \right|^2 \right\}$$

- Using the data model and the second moment formula,

$$E \left\{ \overline{\hat{p}(\omega, \vec{x}_r)} \hat{p}(\omega, \vec{x}_{r'}) \right\} \approx \frac{|\hat{f}(\omega)|^2}{4} \sum_{j,l=1}^{N(\omega)} \phi_l^2(x_\star) \phi_j(r) \phi_j(r') \int dt \mathcal{W}_j^{(l)}(\omega, t, Z).$$

- It is difficult to estimate the source range $z_{\mathcal{A}} = Z/\varepsilon^2$ from $\int dt \mathcal{W}_j^{(l)}(\omega, t, Z) \rightsquigarrow$ **MF will not focus.**



The time integral of the mean Wigner transform

$$\int dt \mathcal{W}_j^{(l)}(\omega, t, Z) \approx \frac{\beta_l(\omega)}{\beta_j(\omega)} \left\{ e^{\Gamma(\omega)Z} \right\}_{jl}$$

- Here $\Gamma(\omega)$ = negative semidefinite matrix

$$\Gamma_{jj} = - \sum_{j \neq l} \Gamma_{jl}, \quad \Gamma_{jl} = \frac{\omega^4 / c_o^4}{4\beta_j\beta_l} \int_{-\infty}^{\infty} \cos [(\beta_j - \beta_l) z] E \{ C_{jl}(0) C_{jl}(z) \} dz$$

- As Z grows columns of $e^{\Gamma(\omega)Z} \rightarrow \text{span}\{(1, \dots, 1)^T\} = \text{null}[\Gamma(\omega)]$

$$\left| \left\{ e^{\Gamma(\omega)Z} \right\}_{jl} - \frac{1}{N(\omega)} \right| \leq O \left(e^{-Z/L_{eq}} \right), \quad -1/L_{eq} = 2\text{-nd eigenval of } \Gamma.$$

Step 4: Imaging at long ranges, where data is incoherent.

Frequency correlation should be exploited for imaging

- Consider

$$\mathcal{F}(\omega, t, r, r') = \int \frac{dh}{2\pi} \hat{p}(\omega, \vec{x}_r) \overline{\hat{p}(\omega - \varepsilon^2 h, \vec{x}_{r'})} e^{-iht}, \quad r, r' \in \mathcal{A}.$$

- Due to frequency decorrelation it self-averages over bandwidth

$$\begin{aligned} \int_{|\omega - \omega_c| \leq B} d\omega \mathcal{F}(\omega, t, r, r') &\approx \int d\omega \int \frac{dh}{2\pi} E \left\{ \hat{p}(\omega, \vec{x}_r) \overline{\hat{p}(\omega - \varepsilon^2 h, \vec{x}_{r'})} \right\} e^{-iht} \\ &\sim \|f\|^2 \sum_{j,l=1}^{N(\omega_c)} \phi_l^2(x_\star) \phi_j(r) \phi_j(r') \mathcal{W}_j^{(l)}(\omega_c, t, Z) \end{aligned}$$

- Here we assumed a bandwidth $O(\varepsilon^2) \ll B \ll O(1)$.

The Wigner transform

- We have $\mathcal{W}_j^{(l)}(\omega, t, Z) = \frac{\beta_l(\omega)}{\beta_j(\omega)} W_j^{(l)}(\omega, t, Z)$ where

$$\left[\partial_Z + \beta_j'(\omega) \partial_t \right] W_j^{(l)}(\omega, t, Z) = \sum_{n \neq j} \Gamma_{jn}(\omega) \left[W_n^{(l)}(\omega, t, Z) - W_j^{(l)}(\omega, t, Z) \right]$$

for $Z > 0$ with initial condition

$$W_j^{(l)}(\omega, t, Z = 0) = \delta(t) \delta_{jl}.$$

- The **source range** $z_A = Z/\varepsilon^2$ is encoded in the t peak of $\mathcal{W}_j^{(l)}(\omega, t, Z)$, i.e. in the cross-correlations $\int d\omega \mathcal{F}(\omega, t, r, r')$.
- We must **estimate the transport speed**. It differs from $\beta_j'(\omega)$.

Range estimation

- Given $p(t, \vec{x}_r)$ at the receivers, compute the cross-correlations

$$\int_{|\omega - \omega_c| \leq B} d\omega \mathcal{F}(\omega, t, r, r') = \int_{|\omega - \omega_c| \leq B} d\omega \int \frac{dh}{2\pi} \hat{p}(\omega, \vec{x}_r) \overline{\hat{p}(\omega - \varepsilon^2 h, \vec{x}'_r)} e^{-iht}$$

- Now **project on the modes** and **backpropagate approximately**

$$\mathcal{R}(\zeta, j) = \int_{\mathcal{A}} dr \phi_j(r) \int_{\mathcal{A}} dr' \phi_j(r') \int_{|\omega - \omega_c| \leq B} d\omega \mathcal{F}(\omega, t = \beta'_j(\omega_c)\zeta, r, r')$$

- This peaks at $\zeta = \zeta_j \neq Z$!
- We estimate the range Z by comparing $\mathcal{R}(\zeta, j)$ with its **theoretical model** $\mathcal{R}^M(\zeta, j; Z^s)$, at source search range Z^s .

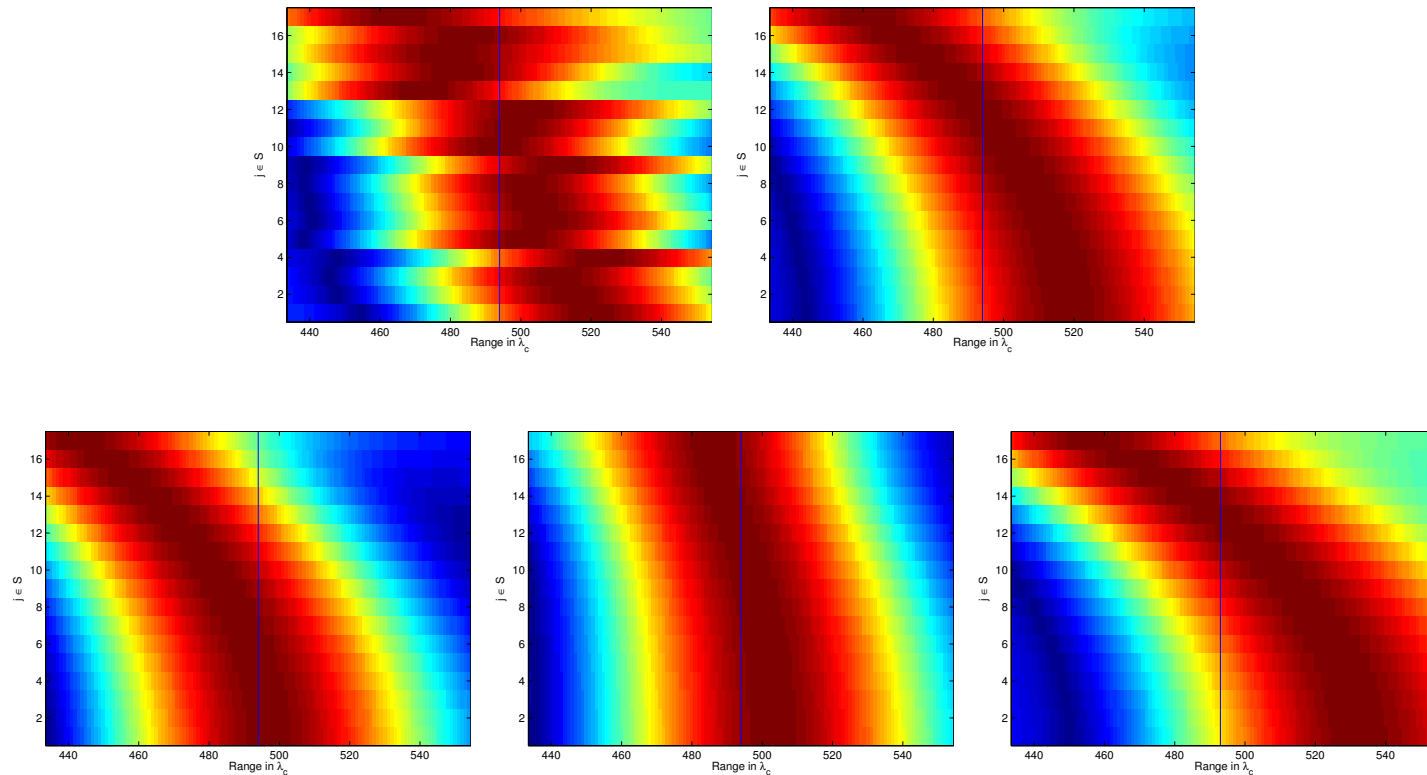
Range estimation

- Estimate Z by minimizing over Z^s

$$\mathbb{O}(Z^s) = \sum_{j \in \mathcal{S}} \int d\zeta \left| \frac{\mathcal{R}(\zeta, j)}{\max_{\zeta'} \mathcal{R}(\zeta', j)} - \frac{\mathcal{R}^M(\zeta, j; Z^s)}{\max_{\zeta'} \mathcal{R}^M(\zeta', j; Z^s)} \right|^2.$$

- Computing $\mathcal{R}^M(\zeta', j; Z^s)$ requires correlation function of the fluctuations. If we don't know it \rightsquigarrow estimate it using a model
 - We have used $E \{ \nu(\vec{x}) \nu(\vec{x}') \} = \sigma^s \mathcal{R} \left(\frac{\vec{x} - \vec{x}'}{\ell^s} \right)$.
 - We found that the range estimation is surprisingly robust with respect to the uncertainty in the above model.

Explanation via numerical simulations

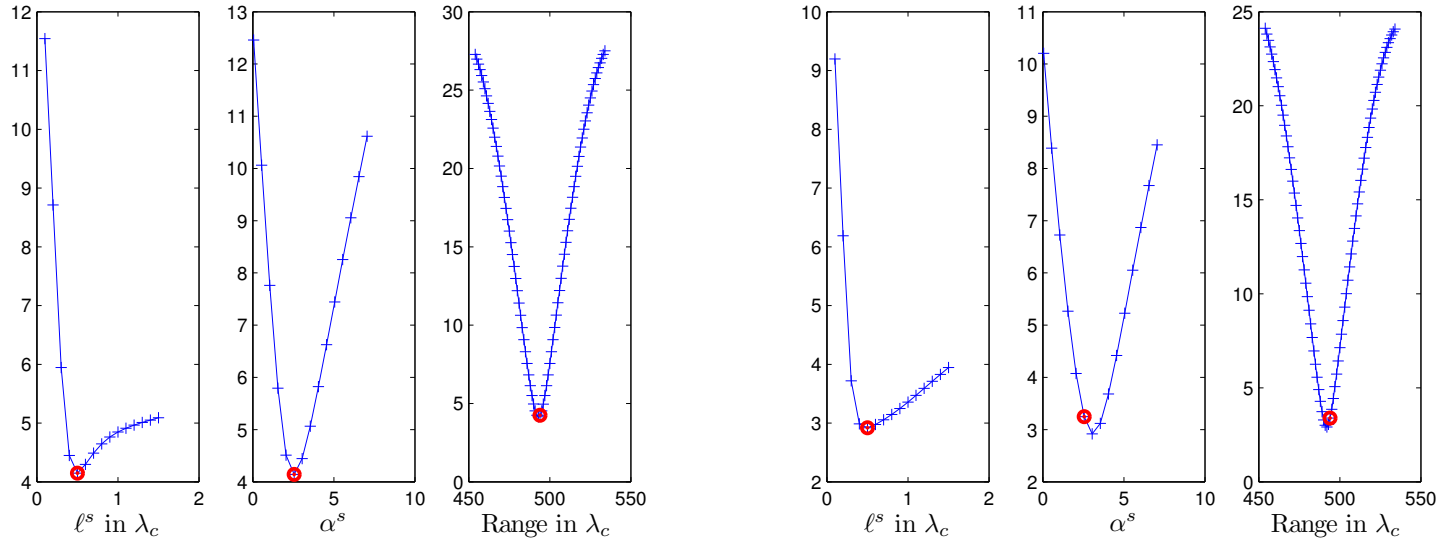


$\varepsilon = 3\%$, central frequency 2.09kHz and bandwidth 0.375kHz.

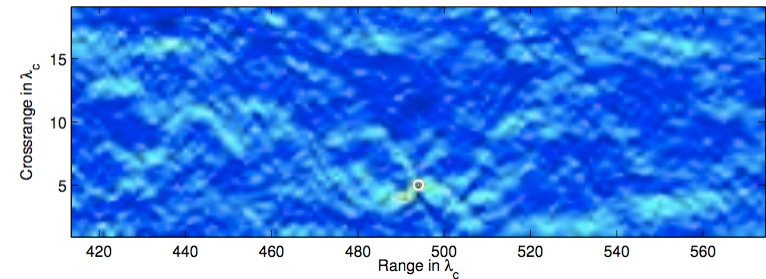
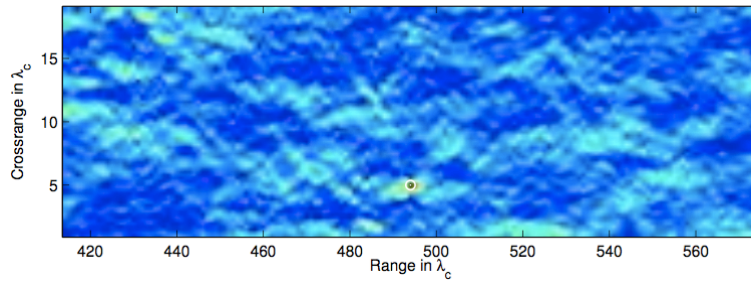
Top row: Left: $\mathcal{R}(\zeta, j)$. **Right:** $\mathcal{R}^M(\zeta, j; Z^*, \sigma^*, \ell^*)$.

Bottom row: $\mathcal{R}^M(\zeta, j; Z^s, \sigma^s, \ell^s)$ for: **Left:** $\frac{Z^s - Z^*}{\varepsilon^2} = -20\lambda_c$.
Middle: $\ell^s = \ell^*/2$. **Right:** $\sigma^s = 1.34\sigma^*$.

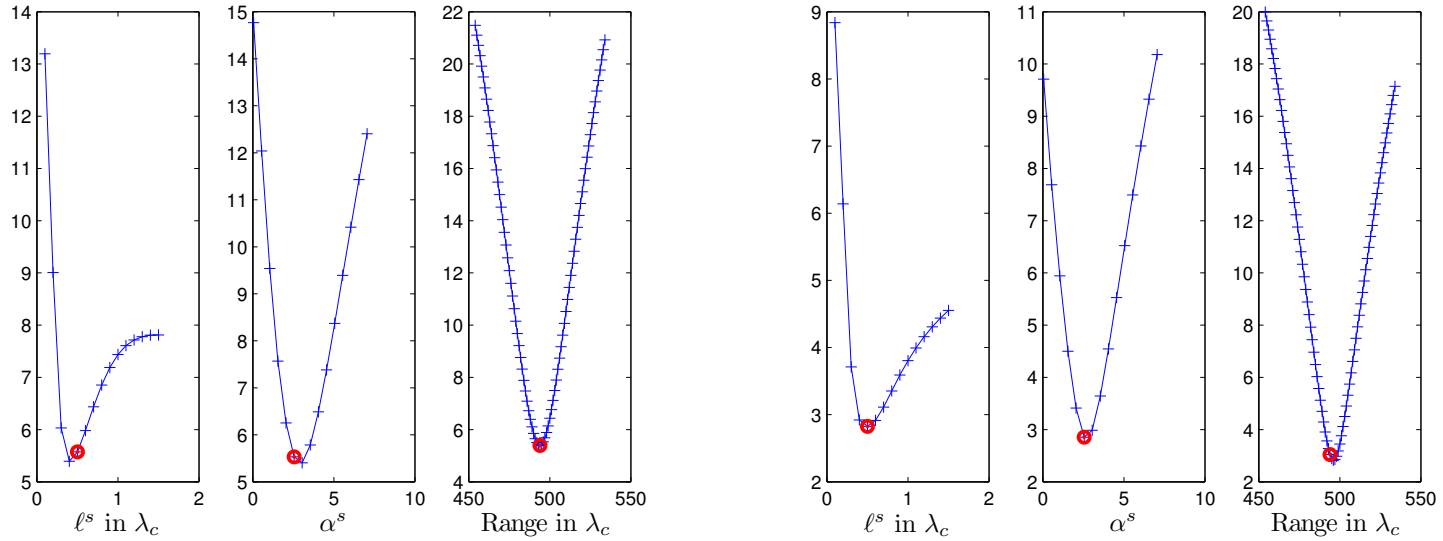
Estimation results. Full aperture, $\varepsilon = 2\%$, central frequency 2.69kHz and bandwidth 0.375kHz



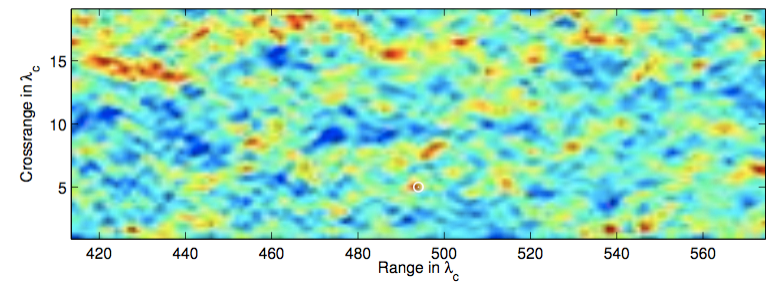
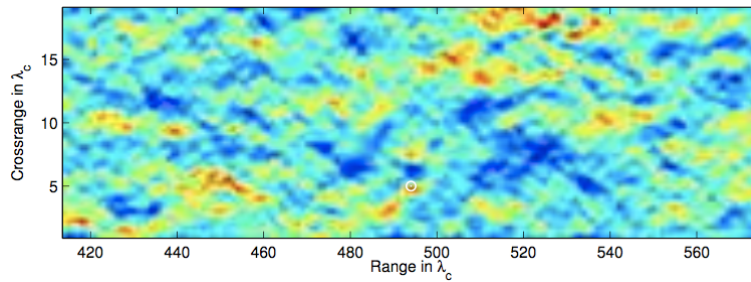
MF



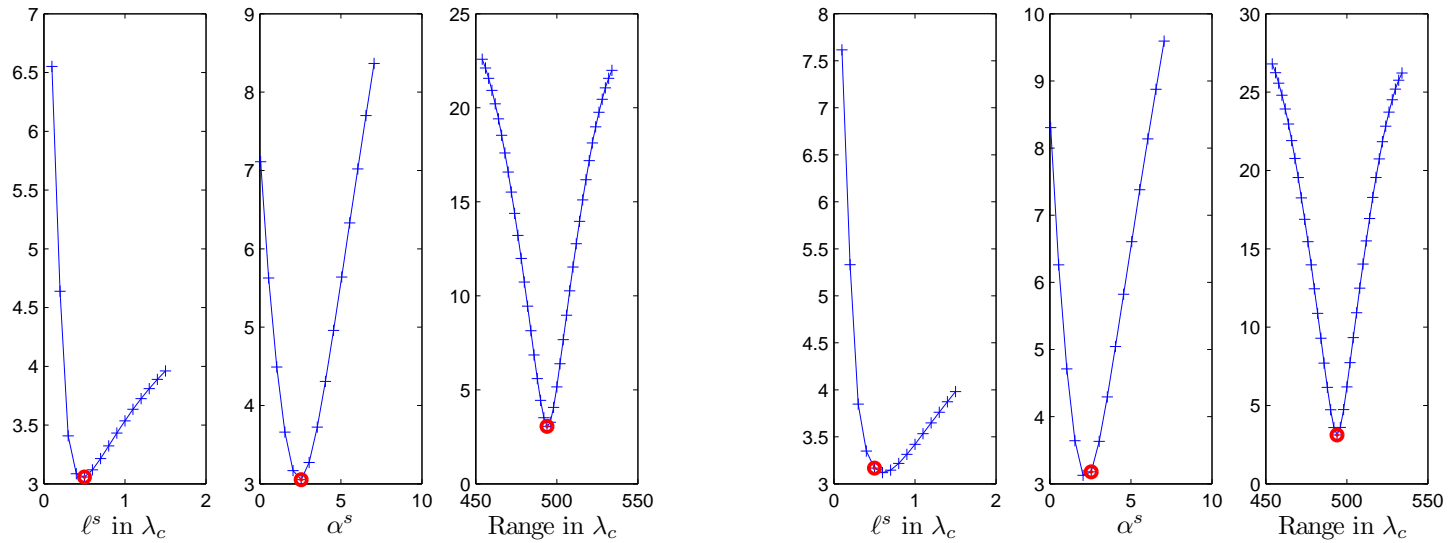
Estimation results. Full aperture, $\varepsilon = 3\%$, central frequency 2.09kHz and bandwidth 0.375kHz



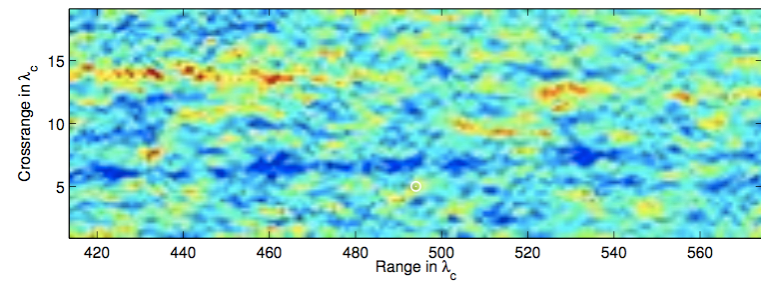
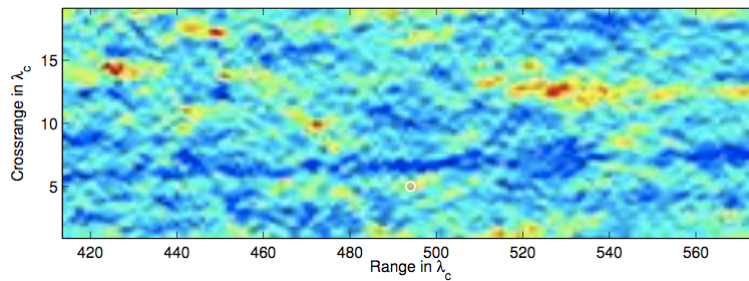
MF



Estimation results. 40% aperture, $\varepsilon = 2\%$, central frequency 2.09kHz and bandwidth 0.375kHz



MF



Cross range estimation

- We compare

$$\mathcal{X}(j) = \int \frac{d\omega}{2\pi} \hat{P}_j(\omega, z_A) \overline{\hat{P}_j(\omega, z_A)}, \quad \hat{P}_j(\omega, z_A) = \int_A dr \hat{p}(\omega, r, z_A) \phi_j(r)$$

with its model

$$\mathcal{X}^M(j; \mathbf{x}^S) \sim \|f_B\|^2 \sum_{q,l=1}^{N(\omega_c)} \mathcal{M}_{jq}^2 \frac{\beta_l(\omega_c)}{\beta_q(\omega_c)} \phi_l^2(\mathbf{x}^S) \left\{ e^{\Gamma^{(c)}(\omega_c) Z^*} \right\}_{ql}$$

for a source at (\mathbf{x}^S, Z^*) .

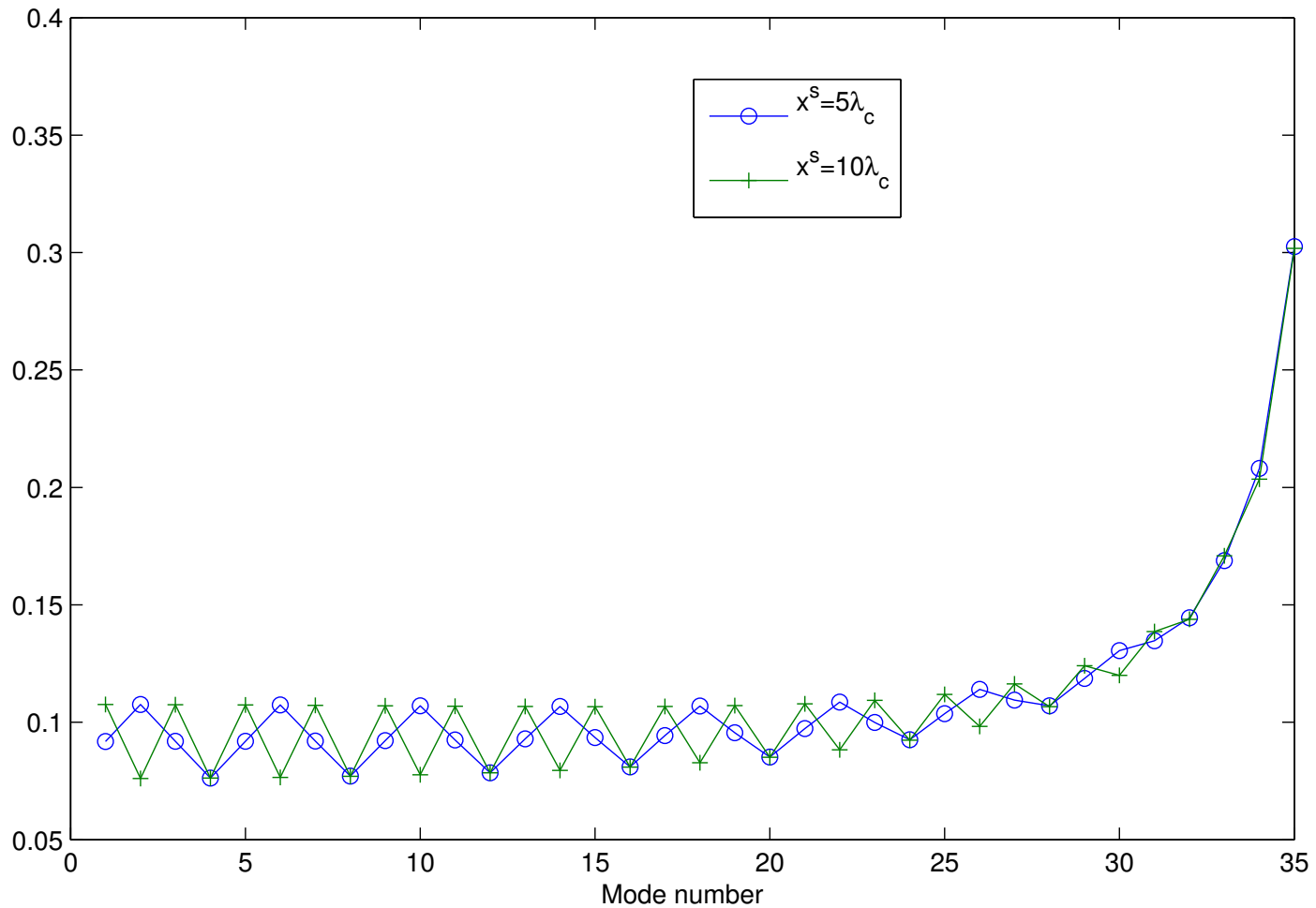
- We estimate the source cross-range by minimizing the misfit.

$$\mathbb{O}(\mathbf{x}^S) = \sum_{j \in \mathcal{S}} \left| \frac{\mathcal{X}(j)}{\langle \mathcal{X}(\cdot) \rangle} - \frac{\mathcal{X}^M(j; \mathbf{x}^S)}{\langle \mathcal{X}^M(\cdot, \mathbf{x}^S) \rangle} \right|^2,$$

where

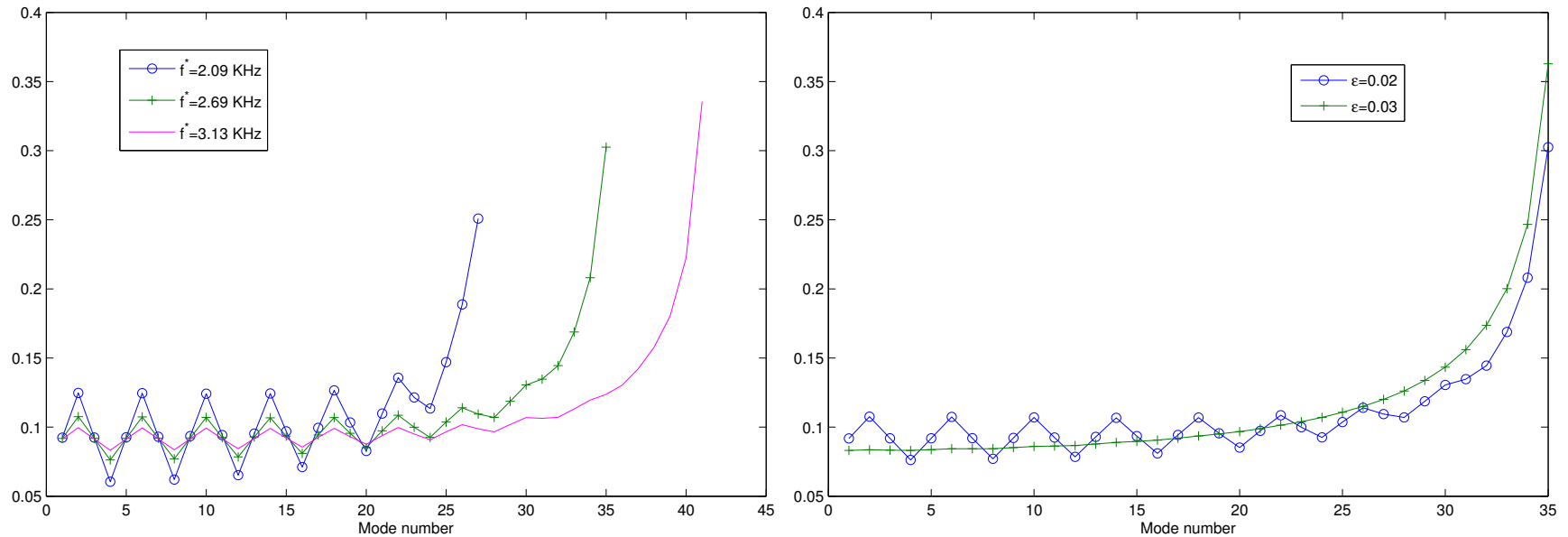
$$\langle \mathcal{X}(\cdot) \rangle = \frac{1}{|\mathcal{S}|} \sum_{j \in \mathcal{S}} \mathcal{X}(j), \quad \langle \mathcal{X}^M(\cdot; \mathbf{x}^S) \rangle = \frac{1}{|\mathcal{S}|} \sum_{j \in \mathcal{S}} \mathcal{X}^M(j; \mathbf{x}^S)$$

Explanation



$\mathcal{X}^M(j; x^s)$ for $x^s = 5\lambda_c$ and $10\lambda_c$, for $\varepsilon = 2\%$, $\omega_c/(2\pi) = 2.69\text{kHz}$ and 0.375kHz bandwidth.

Explanation

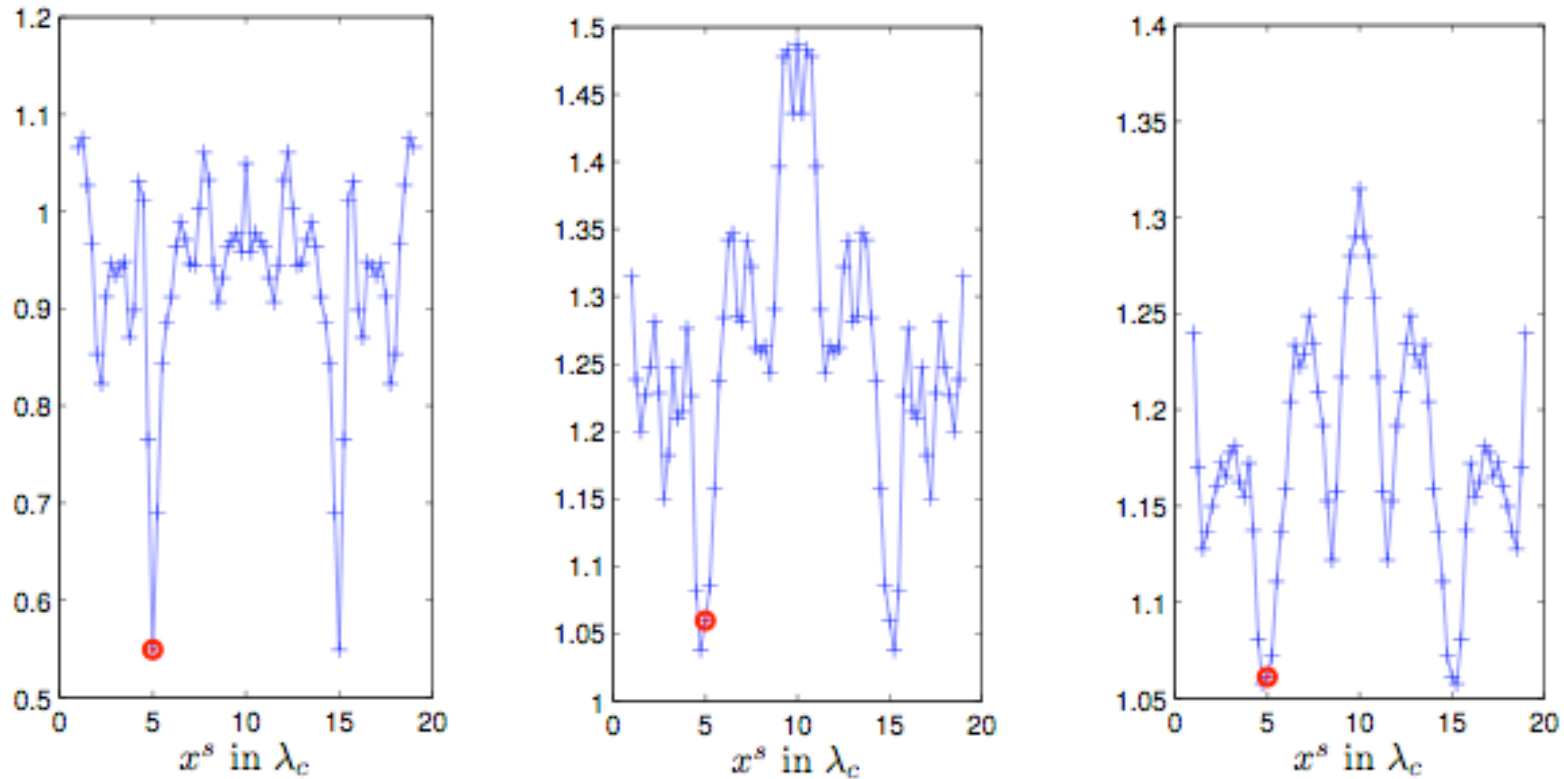


$\chi^M(j; x^s)$ for $x^s = 5\lambda_c$ and full aperture.

Left: $\epsilon = 2\%$, for $\omega_c/(2\pi) = 2.09\text{kHz}$, 2.69kHz and 3.13kHz , respectively.

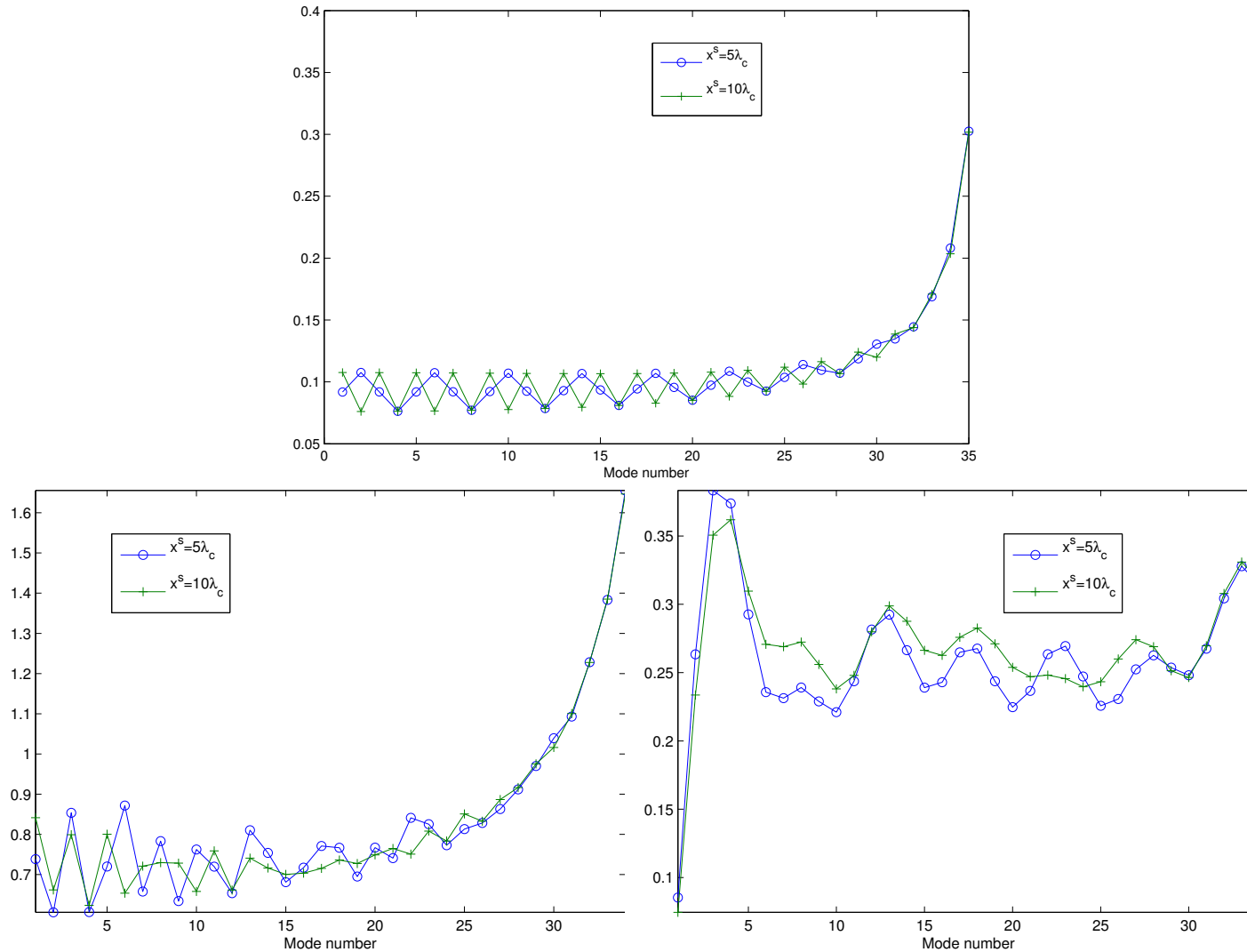
Right: $\omega_c/(2\pi) = 2.69\text{kHz}$ and $\epsilon = 2\%$ and 3% . The bandwidth is 0.375kHz . At 3% there is no cross-range information.

Numerical cross-range estimation at full aperture



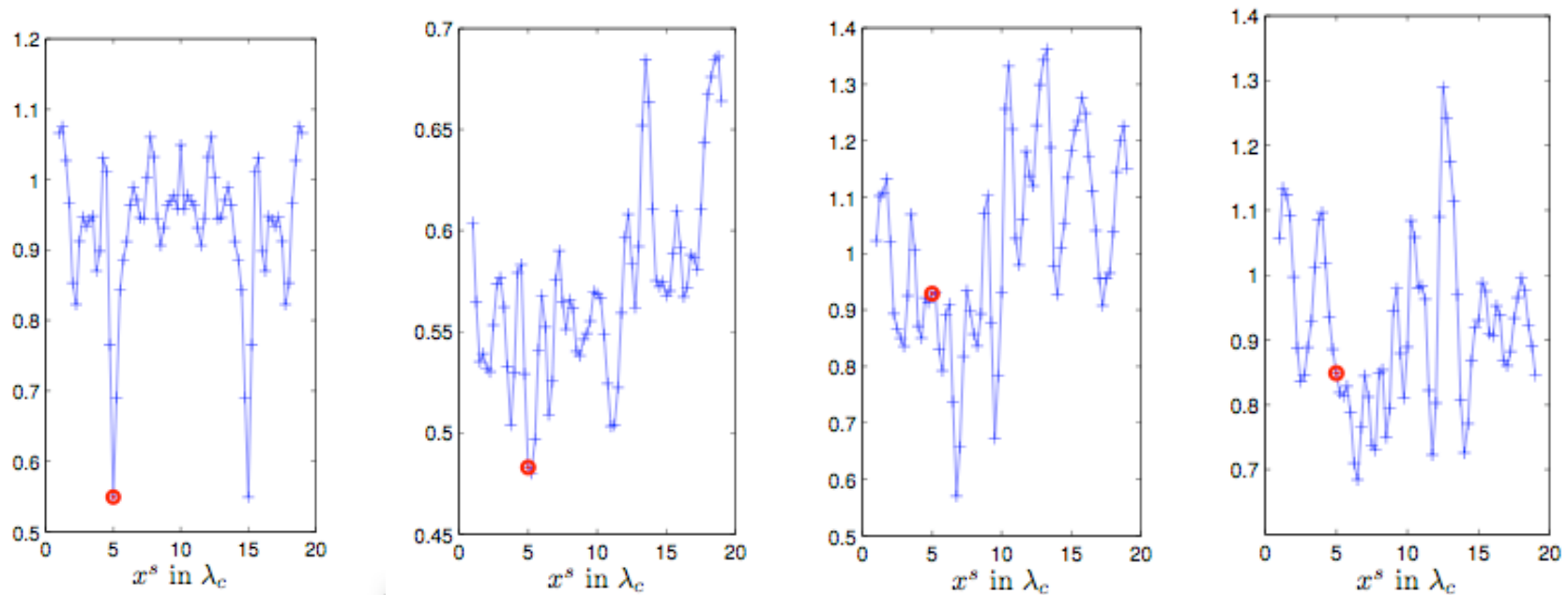
Full aperture cross-range estimation results at $\epsilon = 2\%$, and bandwidth 0.375kHz. **Left:** central frequency 2.69kHz, **middle:** 2.99kHz and **right:** 3.1.3kHz

Partial aperture effects



$\mathcal{X}^M(j; x^s)$ for $x^s = 5\lambda_c$ and $10\lambda_c$, for $\varepsilon = 2\%$, $\omega_c/(2\pi) = 2.69\text{kHz}$ and 0.375kHz bandwidth. **Top:** full aperture $\mathcal{A} = [0, 20\lambda_c]$. **Bottom:** $\mathcal{A} = [0, 12\lambda_c]$ and $\mathcal{A} = [0, 4\lambda_c]$.

Cross-range estimation results. Partial aperture



$\varepsilon = 2\%$, $\omega_c/(2\pi) = 2.69\text{kHz}$ and bandwidth 0.375kHz .

From left: full aperture $\mathcal{A} = [0, 20\lambda_c]$, $\mathcal{A} = [0, 12\lambda_c]$, $\mathcal{A} = [0, 8\lambda_c]$, $\mathcal{A} = [0, 4\lambda_c]$.